Electronic Supplementary Material (ESI) for Nanoscale.

Supporting Information

Catalytically Active Silver Nanoparticles Stabilized on a Thiol-Functionalized Metal-Organic Framework for an Efficient Hydrogen Evolution Reaction

Shamna Muhamed,[a‡] Ravari Kandy Aparna,[a‡] Arun Karmakar,[b] Subrata Kundu,[b] Sukhendu Mandal[a*]

[a] School of Chemistry, Indian Institute of Science Education and Research Thiruvananthapuram, Thiruvananthapuram, Kerala, India-695551; Email: sukhendu@iisertvm.ac.in

[b] Electrochemical Process Engineering (EPE) Division, CSIR-Central Electrochemical Research Institute (CECRI), Karaikudi-630006, Tamil Nadu, India.

[†] Both SM and ARK made equal contributions to this work

Contents

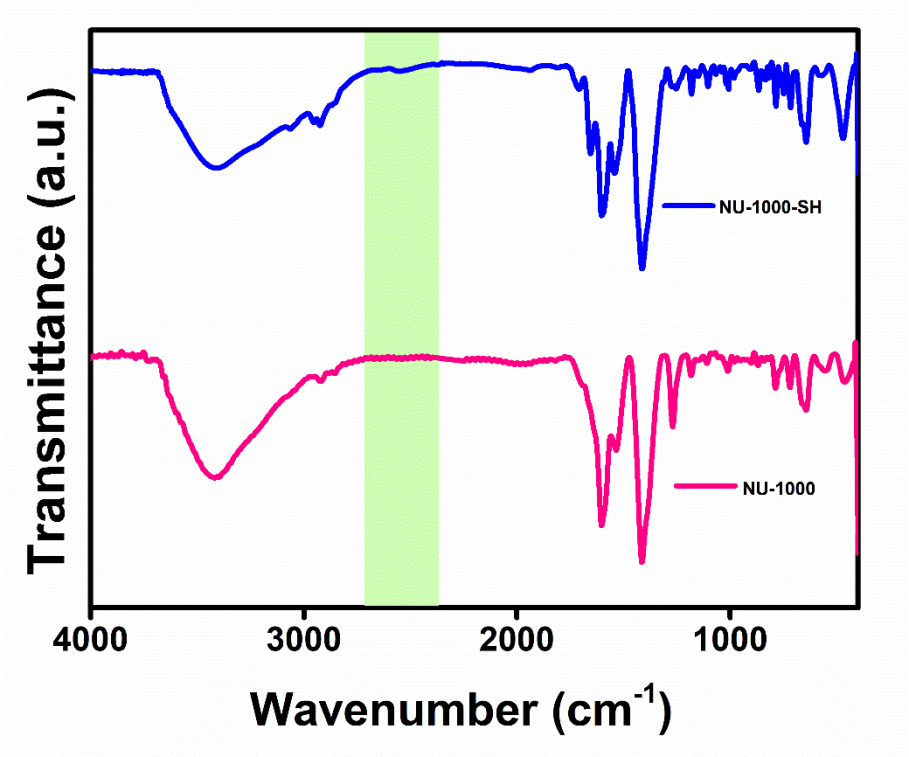

Figure S1. FT-IR spectra of NU-1000 and NU-SH.

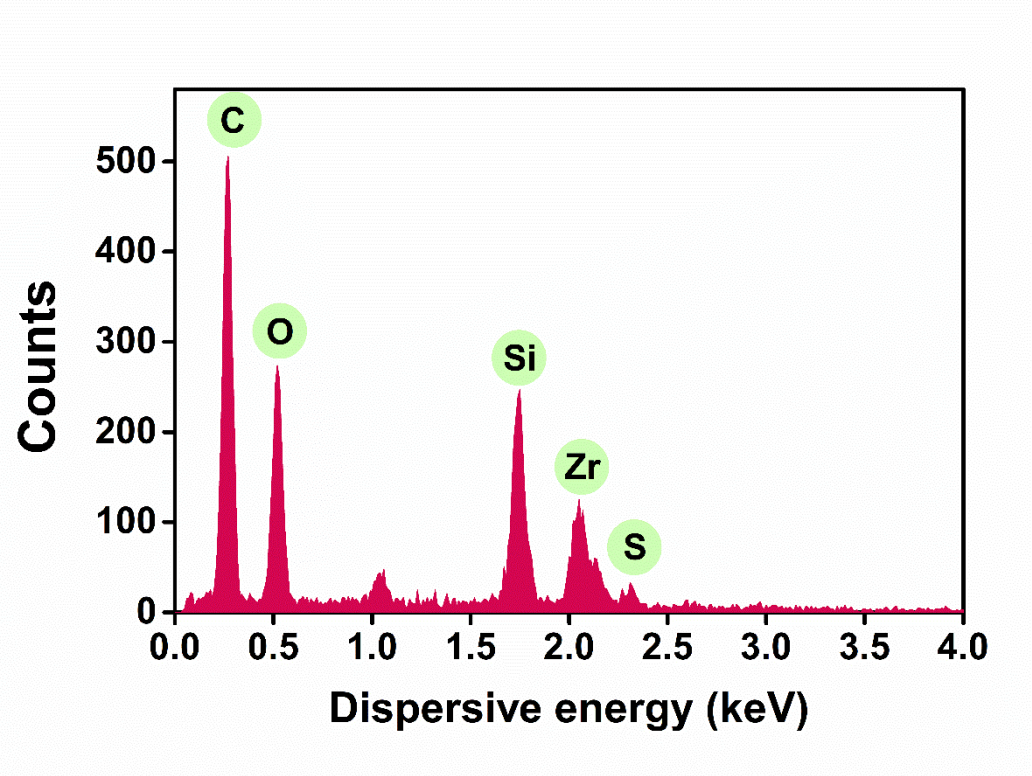

Figure S2. SEM-EDS of NU-SH.

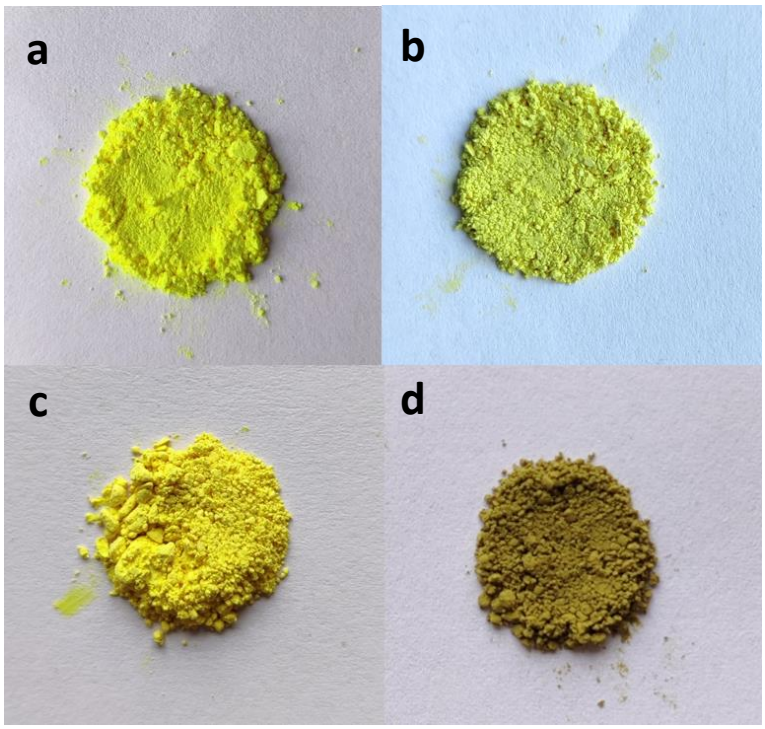

Figure S3. Photographs of the bulk MOF samples. a) NU-1000, b) NU-SH, c) 0.25 $AgNO_3$@NU, d) 0.25 Ag-NU.

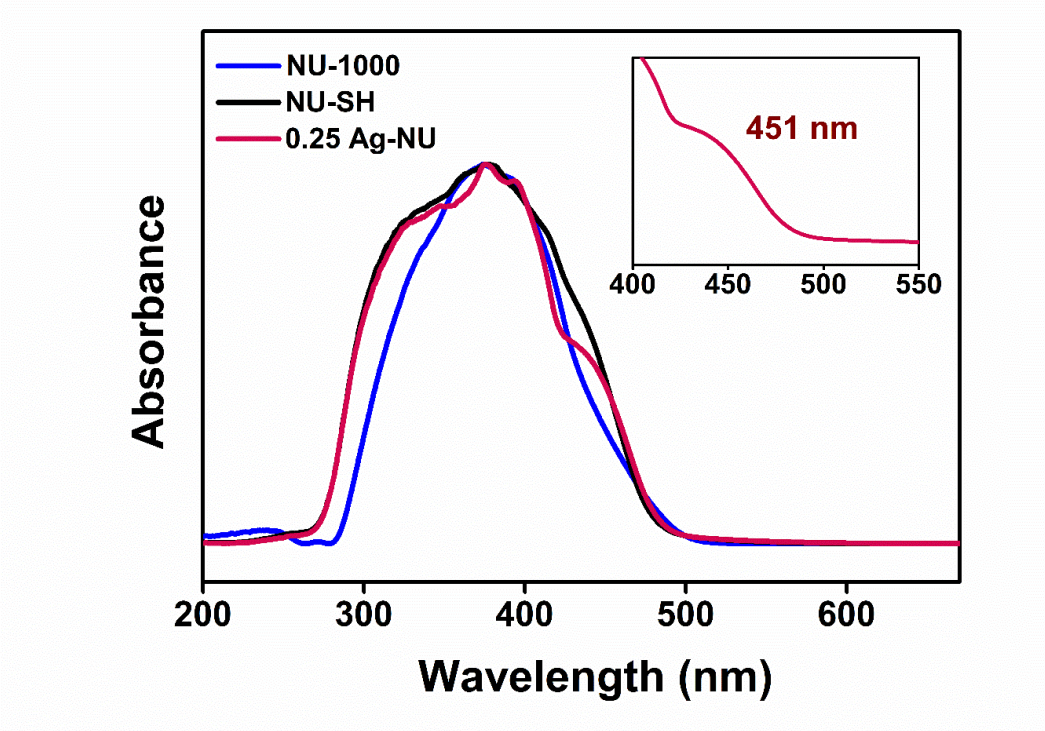

Figure S4. UV-Visible diffuse reflectance spectra of NU-1000, NU-SH and 0.25 Ag-NU.

Table S1. Content of Ag determined by ICP-OES analysis.

Sl. No	Sample	Concentration (ppm)
1	0.1 Ag-NU	0.41
2	0.2 Ag-NU	1.24
3	0.25 Ag-NU	2.13

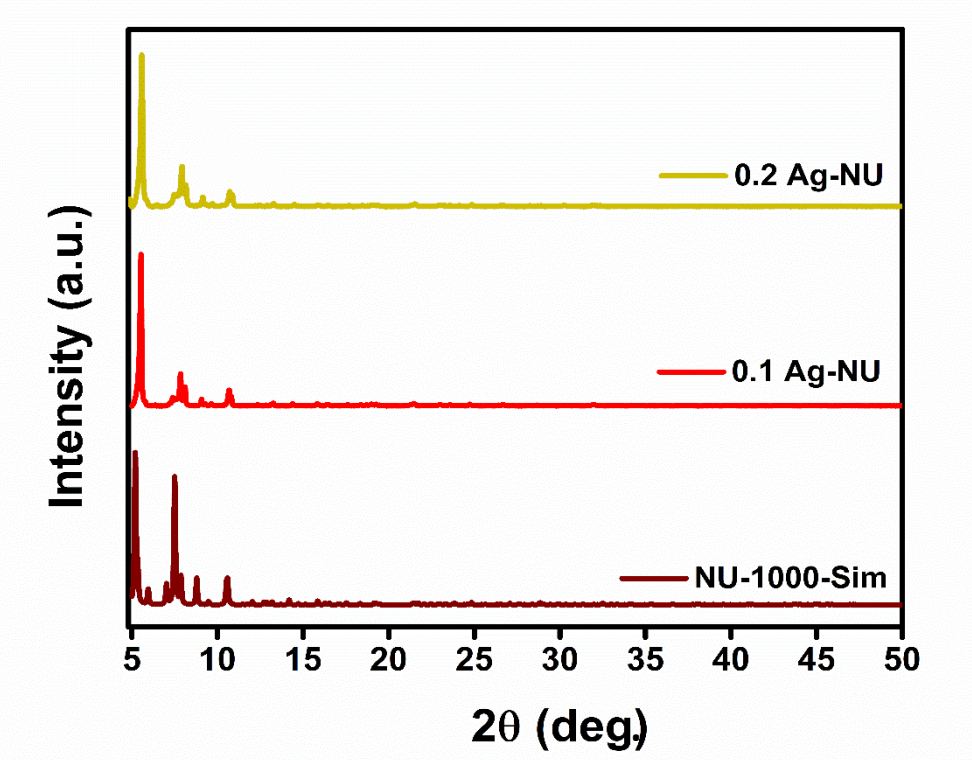

Figure S5. PXRD patterns of simulated NU-1000 and experimental patterns of 0.1 Ag-NU and 0.2 Ag-NU, respectively.

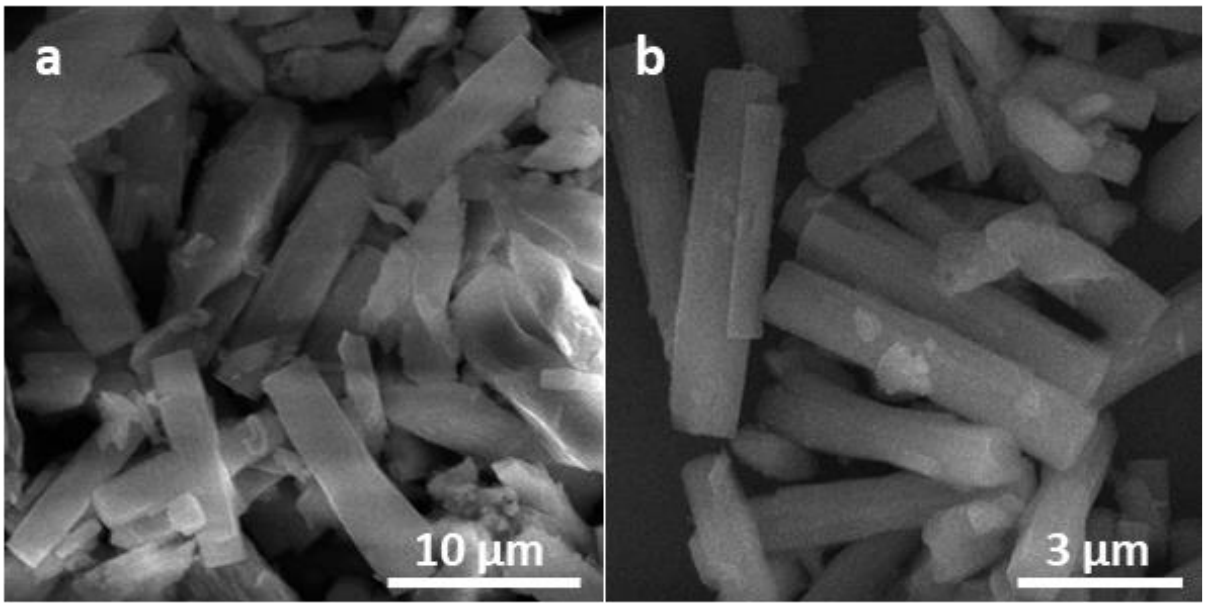

Figure S6. SEM images of a) NU-SH and b) 0.25 Ag-NU.

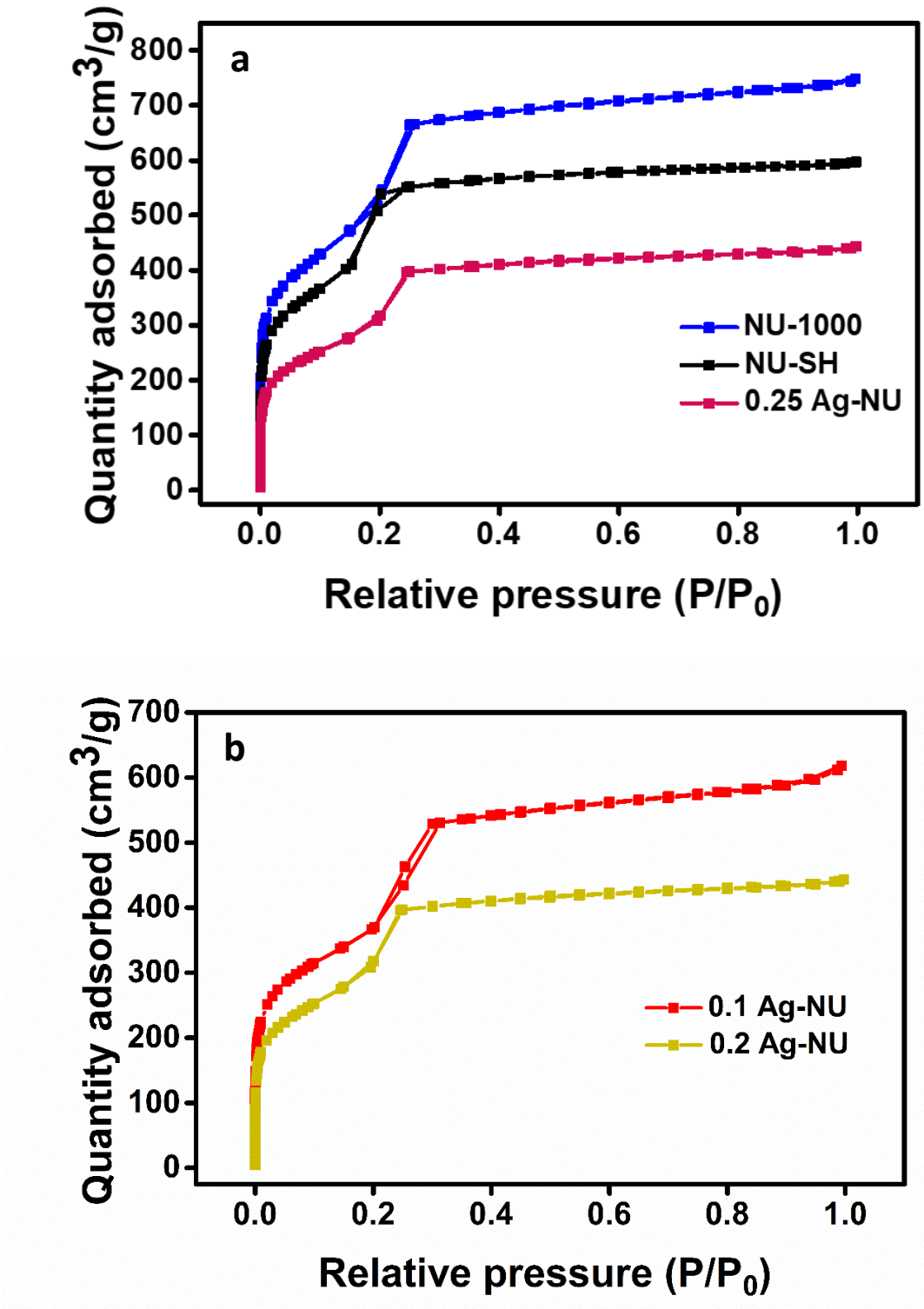

Figure S7. Nitrogen adsorption-desorption isotherms at 77 K of a) NU-1000, NU-SH and 0.25 Ag-NU; b) 0.1 Ag-NU and 0.2 Ag-NU.

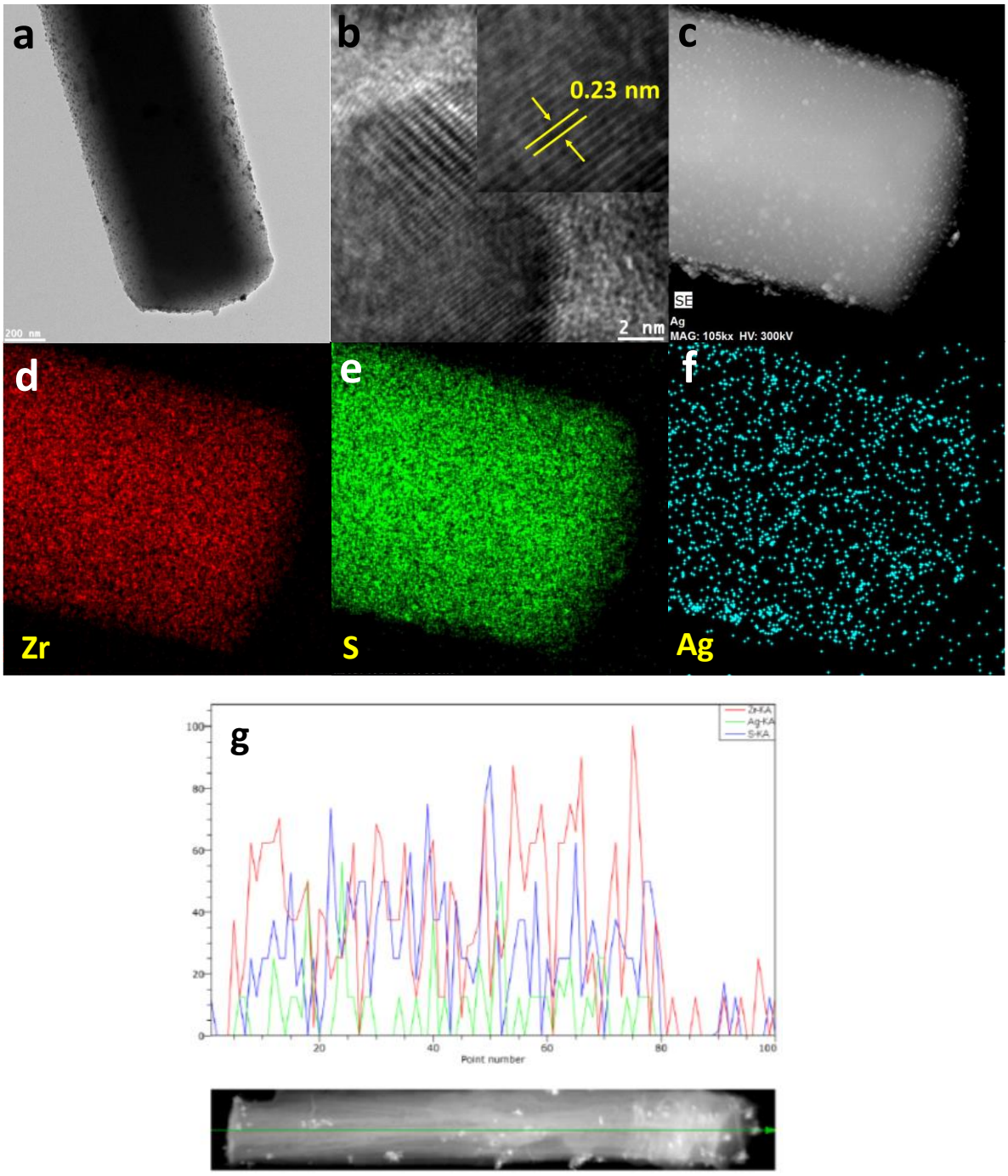

Figure S8. HR-TEM images a) and b) with interplanar spacing (inset), c) STEM-HAADF image and d) - f) elemental mapping images, g) EDS line scan mapping of 0.25 Ag-NU.

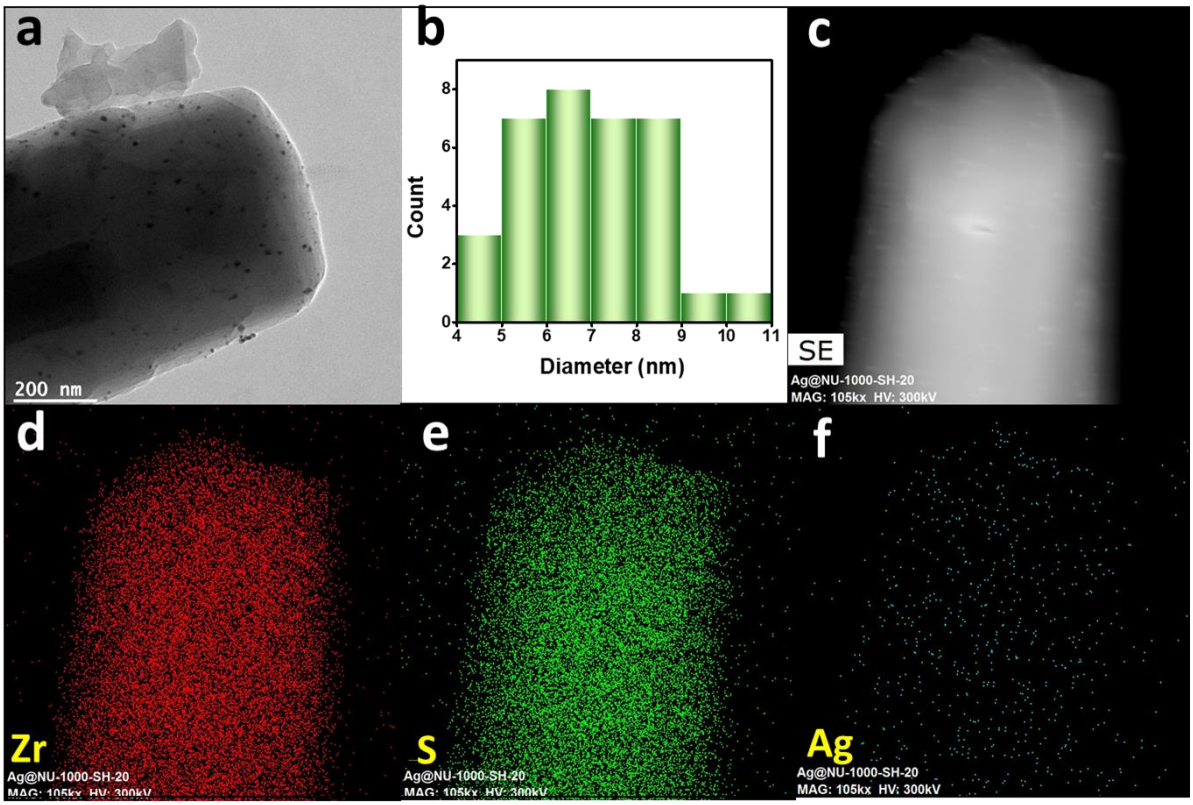

Figure S9. a) HR-TEM micrograph 0.1 Ag-NU, b) size distribution of Ag nanoparticles in 0.1 Ag-NU, c) STEM-HAADF image and d) – f) elemental mapping images of 0.1 Ag-NU.

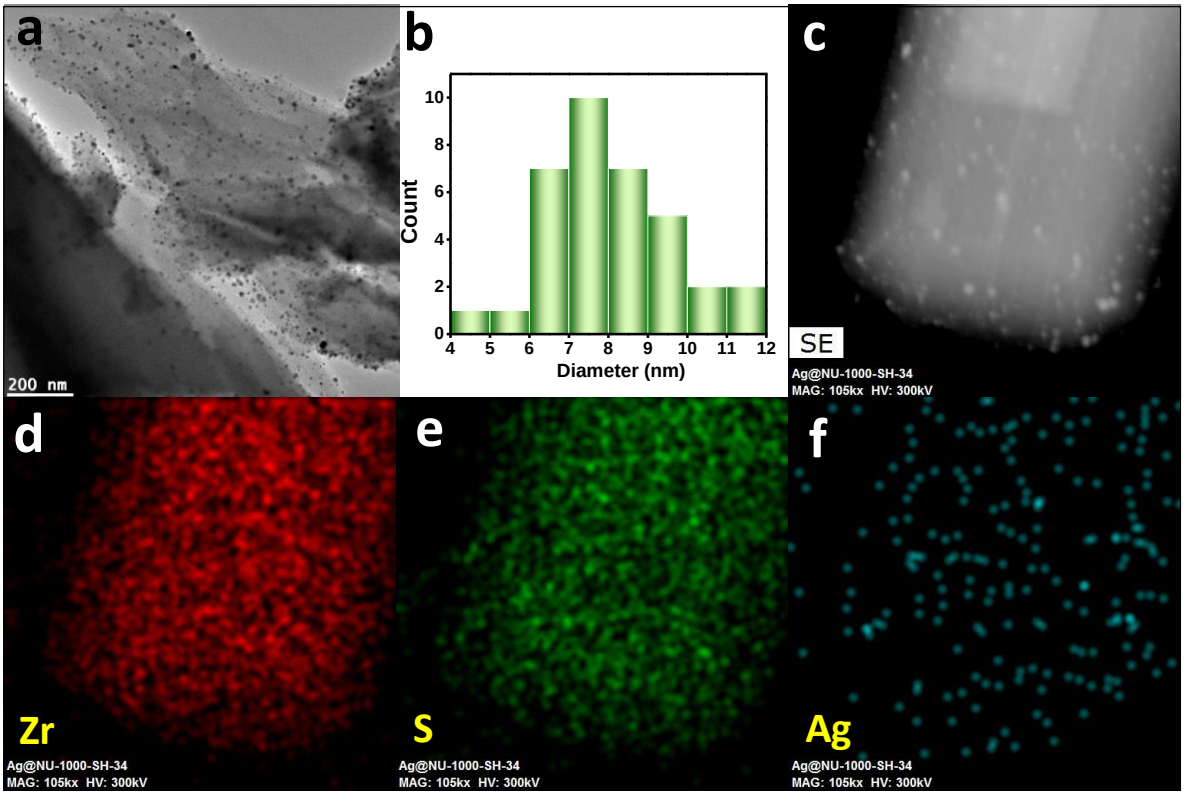

Figure S10. a) HR-TEM micrograph 0.2 Ag-NU, b) size distribution of Ag nanoparticles in 0.2 Ag-NU, c) STEM-HAADF image and d)-f) elemental mapping images of 0.2 Ag-NU.

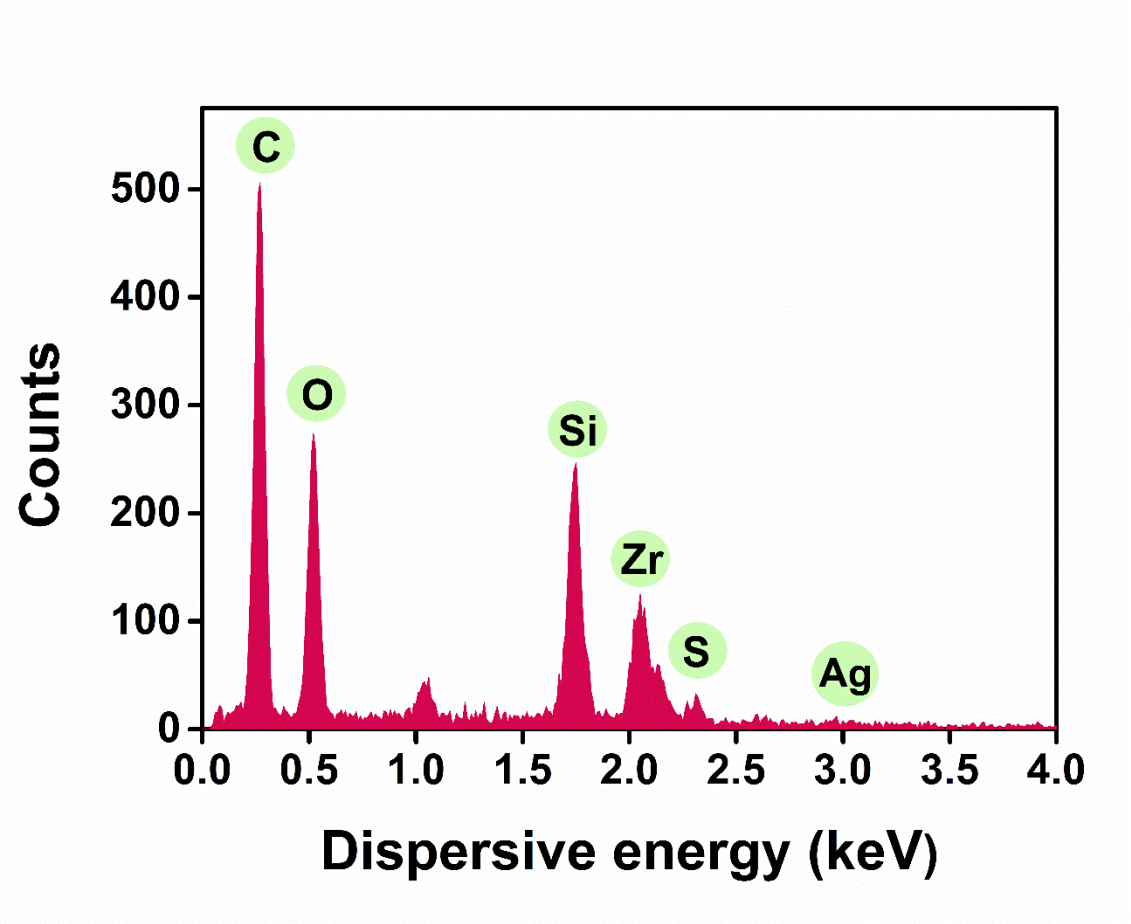

Figure S11. SEM-EDS of 0.25 Ag-NU.

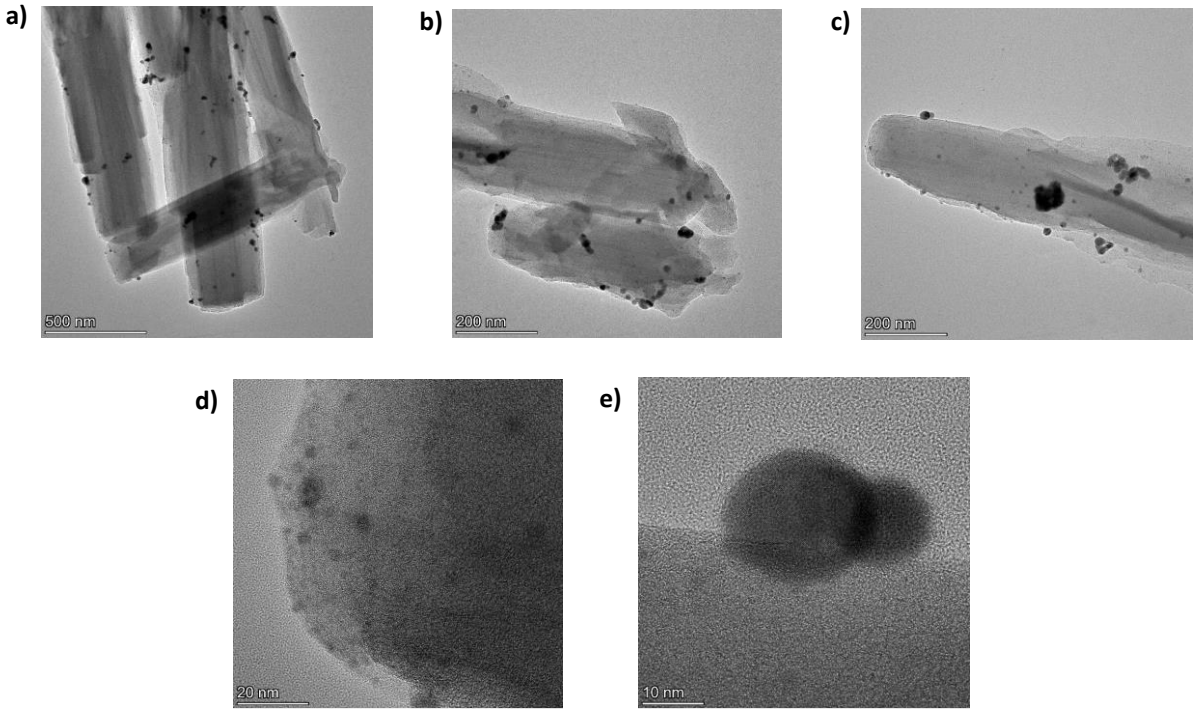

Figure S12. TEM images of 0.3 Ag-NU.

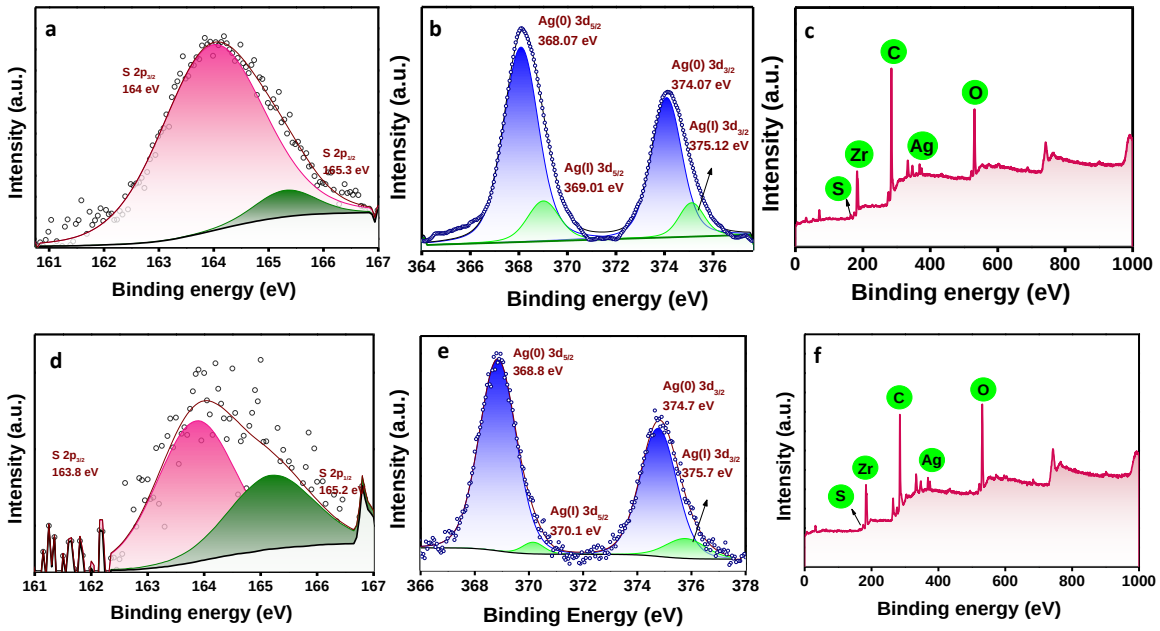

Figure S13. High resolution XPS of a) S 2p, b) Ag 3d, c) survey spectrum of 0.1 Ag-NU, d) S 2p e) Ag 3d and f) survey spectrum of 0.2 Ag-NU.

Table S2. Relative percentages of Ag (0) and Ag (I) in different Ag NP loaded MOF. [a]

Sl. No	Sample	% of Ag (0)	% of Ag (I)
1	**0.1 Ag-NU**	**83.9**	**16.1**
2	**0.2 Ag-NU**	**91.9**	**8.1**
3	**0.25 Ag-NU**	**95.1**	**4.9**

[a] Relative amount of Ag(0) and Ag(I) was calculated based on XPS data

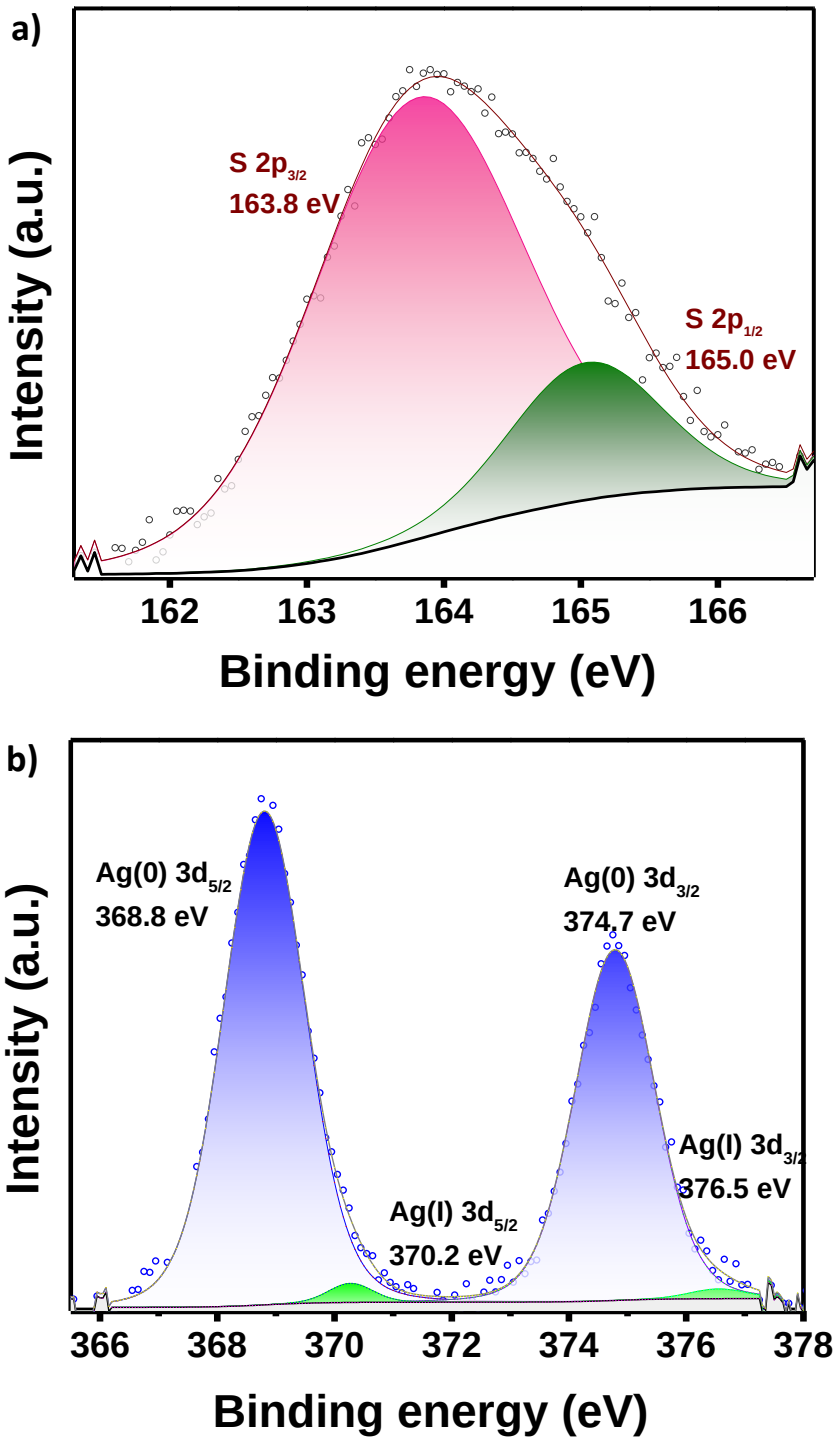

Figure S14. High-resolution XPS of a) S 2p, b) Ag 3d of 0.3 Ag-NU.

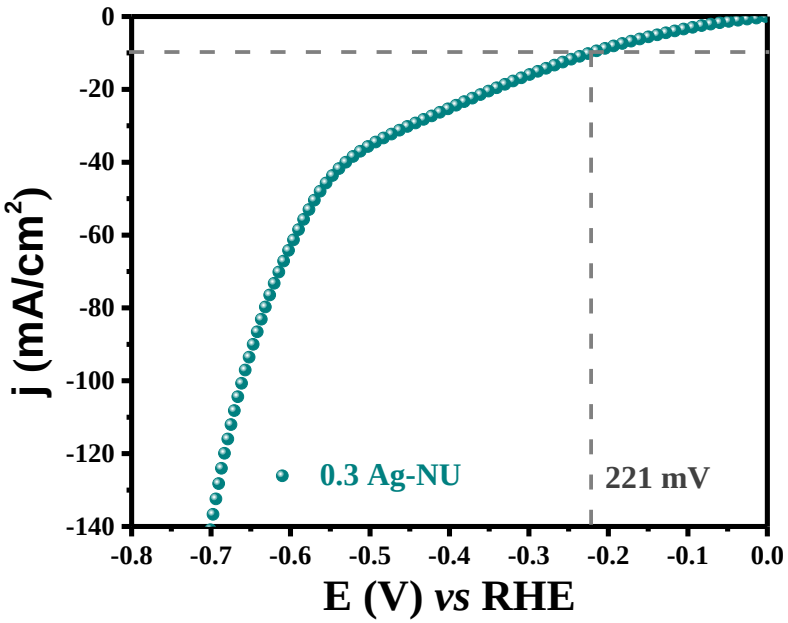

Figure S15. LSV curve of the catalyst with higher Ag loading (0.3 Ag-NU).

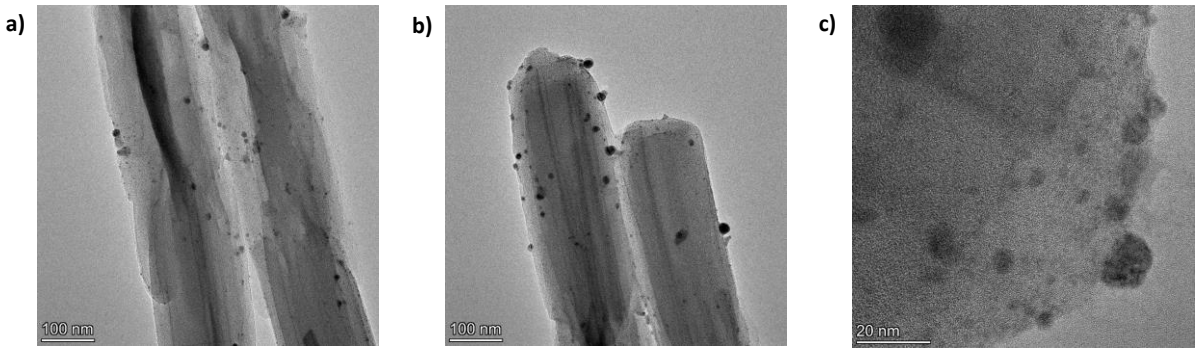

Figure S16. The TEM images of 0.25 Ag-NU without 2-MBA.

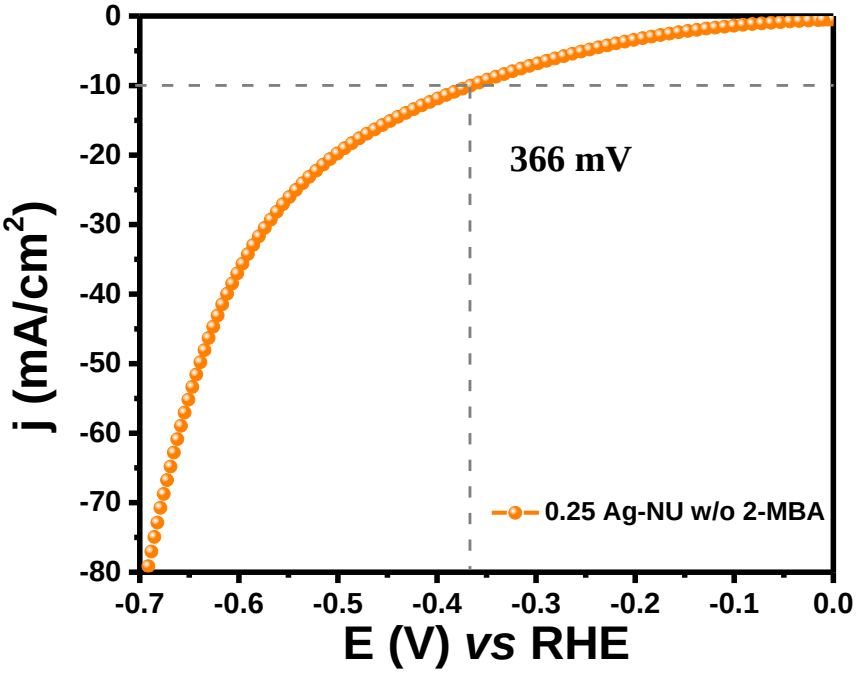

Figure S17. LSV curve of 0.25 Ag-NU without 2-MBA.

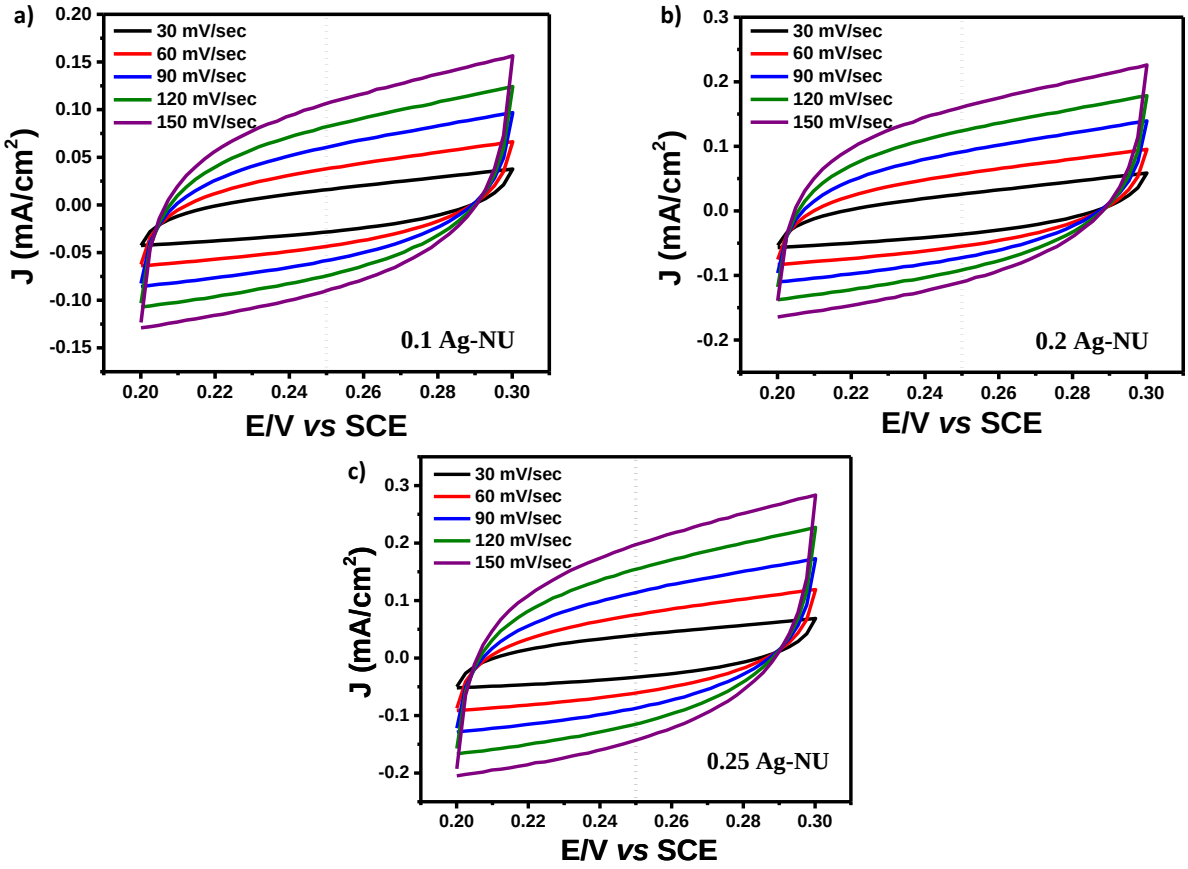

Figure S18. Cyclic voltammety of a) 0.1 Ag-NU b) 0.2 Ag-NU and c) 0.25 Ag-NU conducted in a non-Faradaic region at different scanning rates.

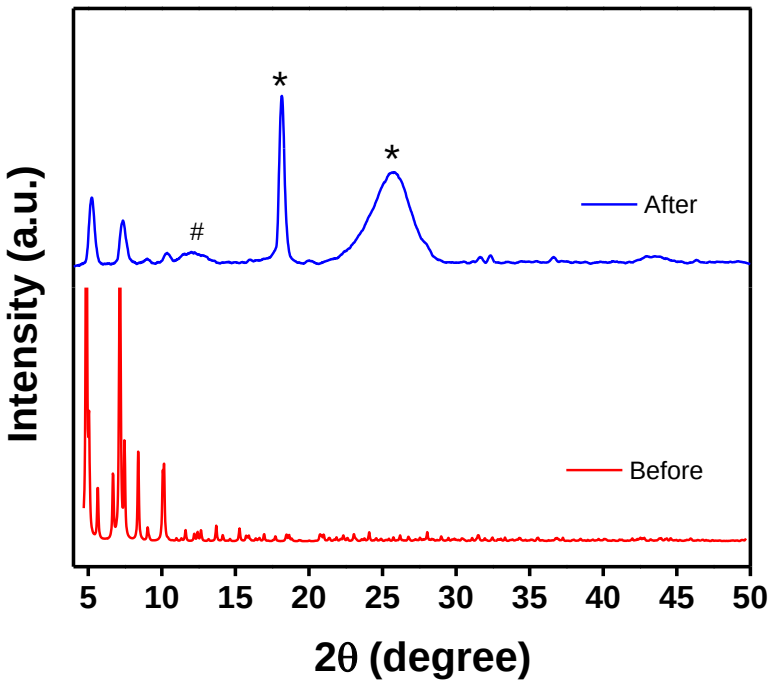

Figure S19. PXRD patterns of 0.25 Ag-NU before and after catalysis. [Peaks marked in asterisk (*) and hash (#) correspond to carbon cloth coated with PTFE and PXRD holder made of polymethylmethacrylate, respectively]

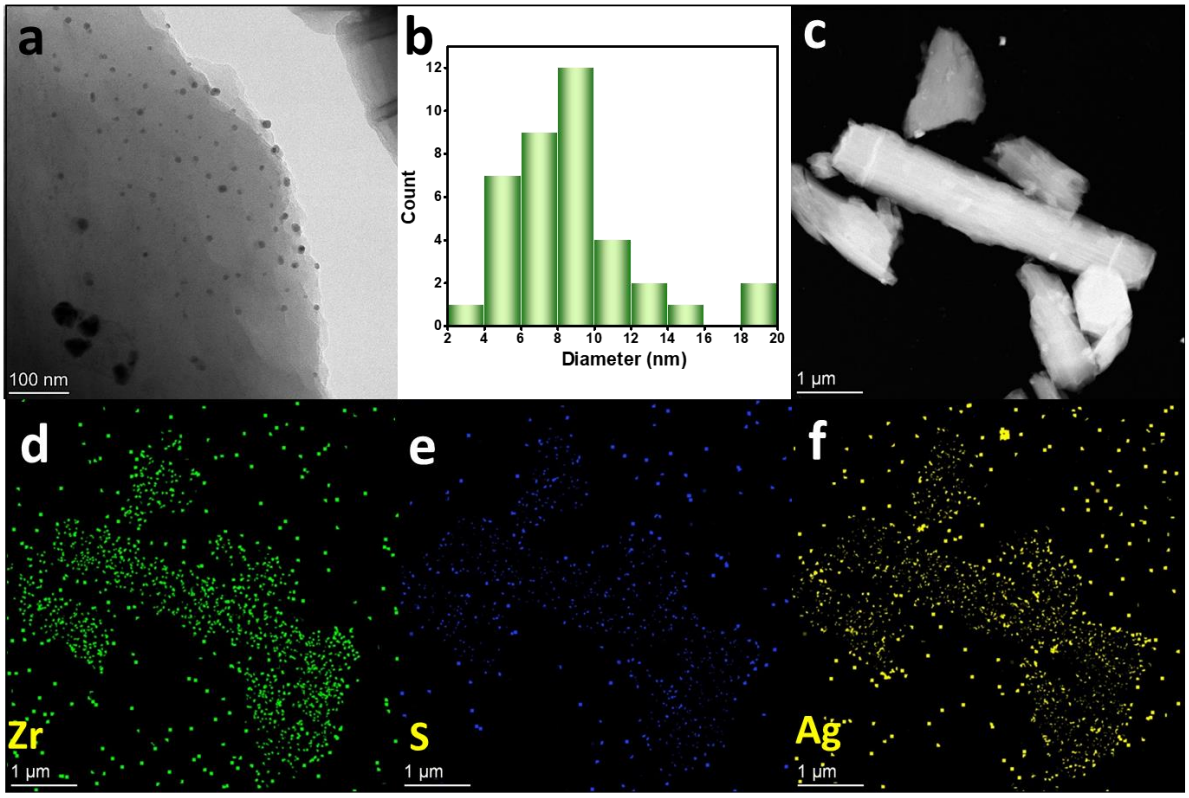

Figure S20. a) HR-TEM micrograph of 0.25 Ag-NU after catalysis, b) size distribution of Ag nanoparticles in 0.25 Ag-NU after catalysis, c) STEM-HAADF image and d)-f) elemental mapping images of 0.25 Ag-NU after catalysis.

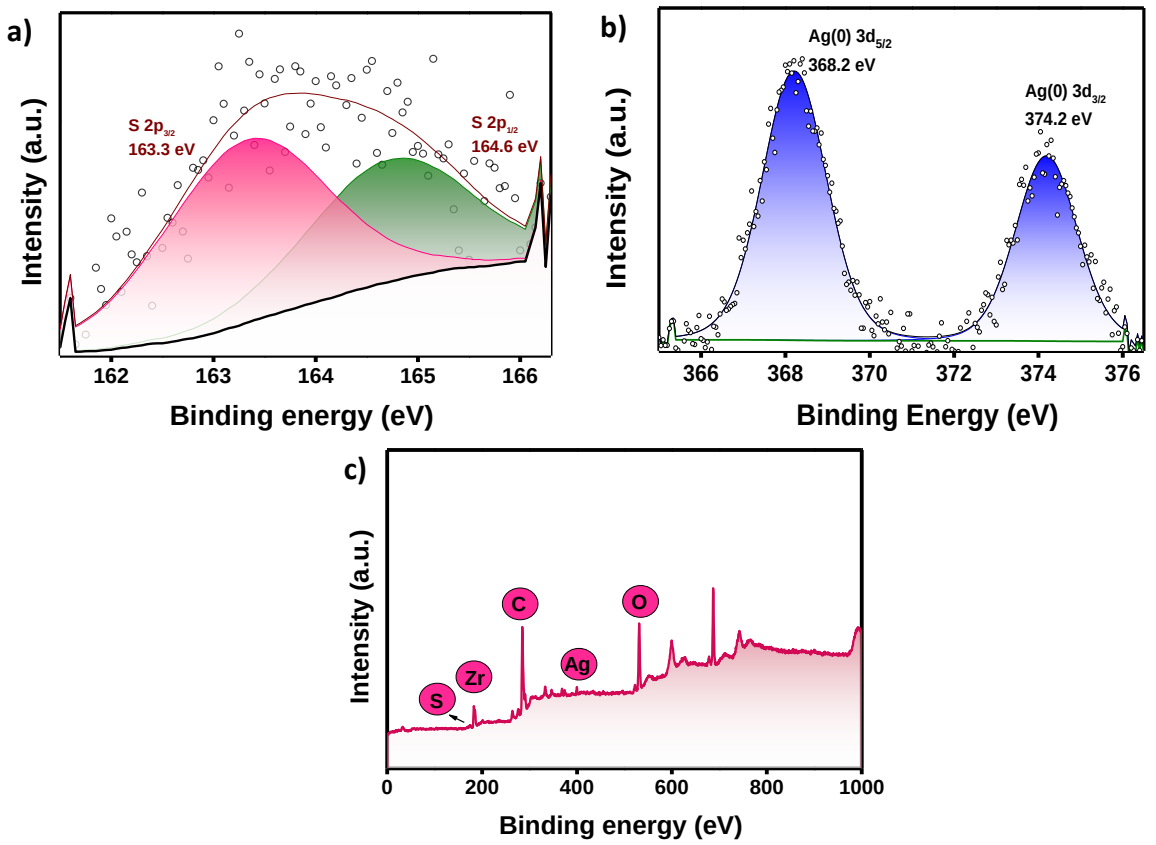

Figure S21. High-resolution XPS of a) S 2p, b) Ag 3d, c) survey spectrum of 0.25 Ag-NU after catalysis.

Determination of Turn-Over Frequency (TOF)

The overall TOF calculation of 0.25 Ag-NU as follows:

TOF = $\left(\frac{total\ hydrogen\ \ turnovers/cm^2}{number\ of\ active\ sites}\right)$

The number of total hydrogen turnovers,

Hydrogen turnover = (j mA/cm^2) $\left(\frac{1\ C/s}{1000\ mA}\right)$ $\left(\frac{1\ mol\ e^-}{96845.3\ C}\right)$ $\left(\frac{1\ mol}{2\ e^-}\right)$ $\left(\frac{6.023\times10^{23}\ molecules\ of\ H_2}{1\ mol\ of\ H_2}\right)$

The number of total hydrogen turnovers was calculated from the current density extracted from the LSV polarization curve.

According to this, the number of total hydrogen turnovers for 0.1 mg of catalyst loading would be

$TON_{(\eta = 100\ mV)}$ (0.25 Ag-NU) = (2.66 mA/cm^2) $\left(\frac{1\ C/s}{1000\ mA}\right)$ $\left(\frac{1\ mol\ e^-}{96485\ C}\right)$ $\left(\frac{1\ mol}{2\ e^-}\right)$ $\left(\frac{6.023\times10^{23}\ molecules\ of\ H_2}{1\ mol\ of\ H_2}\right)$ = 8.3 × 10^{15}

Using the number of total hydrogen turnovers, active site density, and electrochemically active surface area; we converted the current density from the LSV polarization curve into TOF, as:

TOF = $\left(\frac{total\ hydrogen\ \ turnovers/cm^2}{active\ sites}\right)$

*TOF (*0.25 Ag-NU*) =* $\left(\frac{total\ hydrogen\ turnovers/cm^2}{number\ of\ active\ sites}\right)$ = $\left(\frac{8.3\times10^{15}}{4.098\times10^{14}}\right)$ = 20.2 sec^{-1}

From the ICP-OES data:

10^6 µL of solution contains 2.13 mg of Ag

1 µL solution contains = $2.13/10^6$ mg of Ag

34.5 µL solution contains = $2.13\times34.5/10^6$ mg of Ag = 0.0000734 mg = 0.0000000734 g of Ag

107.86 g Ag contain 6.023×10^{23} number of Ag

0.0000000734 = (6.023×10^{23} x 0.0000000734)/107.86 = 4.098 × 10^{14}

Sl no.	Catalyst	Concentration (ppm)	Number of Ag metal	Current density@η = 100 mV (mA/cm^2)	TOF (s^{-1})
1	0.1 Ag-NU	0.41	7.8 × 10^{14}	0.32	12.8
2	0.2 Ag-NU	1.24	2.385 × 10^{15}	1.11	14.5
3	0.25 Ag-NU	2.13	4.098 × 10^{15}	2.66	20.2

Table S3. Comparative HER data for the catalysts with Ag supported on various scaffolds

No.	Catalyst	Electrolyte	Overpotential (mV)	Tafel slope (mV dec^{-1})	Stability	Reference
1	Hb/20Ag@CN	0.5 M H_2SO_4	79 @ 10 $mAcm^{-2}$	155	12 h	1
2	Ag/Ag_2S carbon hybrid structures from pig bristles	0.5 M H_2SO_4	190 @ 10 $mAcm^{-2}$	150	--	2
3	Ti-Ag NPs	0.1 M HCl	130 at 0.1 $mAcm^{-2}$	277	--	3
4	Ag/WO_{3-x}	0.5 M HCl	30 @ 10 $mAcm^{-2}$	40	72 h 5000 cycles	4
5	Ag@haematite	0.5 M H_2SO_4 with MeOH	500 @ 10 $mAcm^{-2}$	72	500 cycles	5
6	$Ag@Fe_3O_4$	0.5 M acetic acid	444 @ 10 $mAcm^{-2}$	123	300 cycles	6
7	(Trigonal MoS_2) 1T-MoS_2@Ag/AuNP	0.5 M H_2SO_4	201 @ 10 $mAcm^{-2}$	53	5000 cycles 10 h	7
8	Ag/vertically aligned MoS_2 modified by galvanic replacement with Pd	0.5 M H_2SO_4	210 @ 10 $mAcm^{-2}$	37	4000 cycles	8

9	MoS_2/Ag/Pd	0.5 M H_2SO_4	215 @ 10 $mAcm^{-2}$	81	30 h	9
10	Ag_2S/rGO composite	0.5 M H_2SO_4	120 @ 10 $mAcm^{-2}$	49.1	1000 cycles	10
11	Ag_2S/MoS_2/RGO	0.5M H_2SO_4	190 @ 10 $mAcm^{-2}$	56	17 h	11
12	Ag/Ag_2S	0.5M H_2SO_4	136 mV@ 10 $mAcm^{-2}$	59	2000 cycles 30 h	12
13	Ag_2S/Ag	0.5M H_2SO_4	199@ 10 mAcm-2	102	1000 cycles	13
14	Ag_2S/CuS	0.5M H_2SO_4	193@ 10 mAcm-2	75	1000 cycles	14
15	0.25 Ag-NU	0.5 M H_2SO_4	165 @ 10 $mAcm^{-2}$	141	24 h 2000 cycles	This work

References

1 D. Rodríguez-Padrón, A. R. Puente-Santiago, M. Cano, A. Caballero, M. J. Muñoz-Batista and R. Luque, *ACS Appl. Mater. Interfaces*, 2020, **12**, 2207–2215.

2 C. M. Cova, A. Zuliani, A. R. Puente Santiago, A. Caballero, M. J. Muñoz-Batista and R. Luque, *J. Mater. Chem. A*, 2018, **6**, 21516–21523.

3 M. A. Amin, S. A. Fadlallah and G. S. Alosaimi, *Int. J. Hydrogen Energy*, 2014, **39**, 19519–19540.

4 Y. Ren, Z. Chen and X. Yu, *Chem. - An Asian J.*, 2019, **14**, 4315–4321.

5 P. Chaudhary and P. P. Ingole, *Int. J. Hydrogen Energy*, 2018, **43**, 1344–1354.

6 M. Sahu, M. Shaikh, A. Rai and K. V. S. Ranganath, *J. Inorg. Organomet. Polym. Mater.*, 2020, **30**, 1002–1007.

7 J. Wang, W. Fang, Y. Hu, Y. Zhang, J. Dang, Y. Wu, H. Zhao and Z. Li, *Catal. Sci. Technol.*, 2020, **10**, 154–163.

8 I. Gerlitz, M. Fiegenbaum-Raz, M. Bar-Sadan, H. Cohen, A. Ismach and B. A. Rosen, *ChemElectroChem*, 2020, **7**, 4224–4232.

9 M. D. Sharma, C. Mahala and M. Basu, *ChemistrySelect*, 2019, **4**, 378–386.

10 C. Zhao, Z. Yu, J. Xing, Y. Zou, H. Liu, H. Zhang and W. Yu, *Catalysts*, 2020, **10**, 1–12.

11 G. Solomon, R. Mazzaro, S. You, M. M. Natile, V. Morandi, I. Concina and A. Vomiero, *ACS Appl. Mater. Interfaces*, 2019, **11**, 22380-22389.

12 H. Xu, X. Niu, Z. Liu, M. Sun, Z. Liu, Z. Tian, X. Wu, B. Huang, Y. Tang and C. H. Yan, *Small*, 2021, **17**, 1–12.

13 M. Basu, R. Nazir, C. Mahala, P. Fageria, S. Chaudhary, S. Gangopadhyay and S. Pande, *Langmuir*, 2017, **33**, 3178–3186.

14 H. Ren, W. Xu, S. Zhu, Z. Cui, X. Yang and A. Inoue, *Electrochim. Acta*, 2016, **190**, 221–228.